Surface Engineering of Graphene for High Performance Supercapacitors

Ziyin Lin[1], Yan Liu[1], Yagang Yao[1], Owen J. Hildreth[1], Zhuo Li[1], Kyoungsik Moon[1], Joshua C. Agar[1] and Chingping Wong[1,2] *
[1]School of Materials Scicence and Engineering, Georgia Institute of Technology
771 Ferst Drive, Atlanta, GA, USA 30332
[2] College of Engineering, the Chinese University of Hong Kong, Hong Kong
[*]Phone: (404) 894-8391 Fax: (404) 894-9140 Email: cp.wong@mse.gatech.edu

Abstract

A solvothermal method was used to synthesize functionalized graphene, which exhibits an ultrahigh capacitance. This solvothermal method allows a fine control of the density of functionalities on graphene surface. The structure of resulting functionalized graphene is characterized by X-ray photoelectron spectroscopy (XPS), thermal gravimetric analysis (TGA), FTIR and Raman. Pseudocapacitance is provided by functionalities on graphene surface, such as carboxyl, carbonyl and hydroxyl. The significance of these functional also includes improving the wetting properties of electrode material, especially for supercapacitors using aqueous electrolyte. However, there is a penalty for functionalities since these oxygen-containing functional groups will disrupt the π-conjugated system and lower the electrical conductivity. Therefore for functionalized graphene as supercapacitor, a tradeoff exists between the high psudeocapacitance and low conductivity, both are arising from the surface functionalities. Our systematic study shows a successful control of the density of functionalities, which is essential to achieve high performance of graphene-based supercapacitors. The capacitance of graphene is measured in a three electrode system using cyclic voltammetry (CV) and galvanostatic charging/discharging techniques. At a proper reduction condition, a high capacity of 276 F/g was achieved at a discharging current of 0.1 A/g in H_2SO_4 solutions. The superior capacitive performance of functionalized graphene demonstrates the importance of surface property engineering, which will greatly promote the study and application of graphene-based supercapacitors.

1. Introduction

Electrochemical double layer capacitor (EDLC), also called supercapacitor, is a novel energy storage device, which has advantages of high power density, long cycle life and low maintenance. It has promising applications in hybrid electric vehicles and portable electronics. Lots of researches have been dedicated to improve the capacity of supercapacitors, among which there is a special focus on new electrode materials, the central part of supercapacitors. [1]

Graphene is an ideal candidate for electrode materials due to its outstanding properties such as high surface area, good electrical conductivity and open porous structure.[2] However, the specific capacitances of graphene in most works on graphene-based supercapacitors are significantly lower than the theoretical value (~ 550 F/g [3]). The unsatisfactory performance of graphene is because severe aggregations of graphene due to strong van der Waals force, and poor wetting property between non-polar graphene and polar electrolytes. In order to improve the capacitance of graphene-based supercapacitor, pseudocapacitance has been introduced by incorporating chemical reactions into the charge/discharge process. The chemical reaction is usually provided by metal oxide and electrical conducting polymers, which form composite materials with graphene. For example, MnO_2/graphene [4] and poly aniline (PANI)/graphene [5] have been synthesized which exhibit higher specific capacitance than pure graphene. However, issues of composite materials, such as poor rate performance and short cycle life, limit the application of these materials.

In this report, we propose to use oxygen-containing functional groups dispersed on the surface of graphene to improve the performance of graphene-based supercapacitors. Surface functional groups, such as carbonyl and hydroxyl, are able to provide pseudocapacitance similar to metal oxide and conducting polymers. Moreover, these functional groups are polar and hydrophilic, which can improve the wetting between graphene and polar electrolytes and prevent aggregations of graphene sheets. However, there is a penalty of losing electrical conductivity due to disruption of conjugated system of graphene. Therefore, the density of functionalities as well as their distributions needs to be carefully controlled.

The controlled preparation of functonalized graphene (fG) is very challenging for simple direct oxidation of graphene. Due to the inert nature of graphite, the starting material to be exfoliated to produced graphene, harsh conditions are usually used to introduce oxygen-containing groups. For example, the Hummers method uses concentrated H_2SO_4 and $KMnO_4$;[6] the Staudenmaier method use concentrated HNO_3 and H_2SO_4 as well as $KClO_3$.[7] Under these conditions, it is unlikely to finely control the density and distribution of functionalities. Therefore, the reduction of the graphene oxide (GO), a highly oxidized form of graphene, is more practical and controllable. Although there is a resistance of removing all oxygen from GO, it is still possible to control the oxygen content within a wide range. However, current researches on GO reduction all aim to achieve an efficient and complete reduction. Controllable reduction and its applications have been less explored.

In this work, a mild solvothermal method was employed to reduce GO. Our method does not employ any typical reducing agent and use a relative low temperature (150 °C). The density of functionalities was controlled by changing the reduction time. At an optimized condition, a specific capacitance up to 276 F/g was achieved. Surface functionalities on fG are critical for achieving superior supercapacitive property, which will be discussed in detail in

terms of their influence on electrical conductivity, pseudocapacitance, wetting properties and aggregations.

2. Experimental

2.1. Synthesis

GO was prepared by hummer's method.[6] In a typical experiment, 1g graphite flake (230U from Asbury) was dispersed in a solution containing $NaNO_3$ (1 g) and concentrated H_2SO_4 (100 mL) solution which is placed in an ice bath. 6 g $KMnO_4$ was then slowly added to the solution, while maintaining the temperature below 20 °C. The mixture was stirred in the ice bath for 2 hours, and placed in another 35 °C water batch for 0.5 hour. After that, 46 mL 70 °C water was added dropwise. The solution was heated up to 98 °C. 140 mL 70 °C water was then added, followed by 20 mL 30 wt % hydrogen peroxide solution, which was used to terminate the reaction. The product was separated by filtration and washed with water to remove the excessive acid and inorganic salts. The resulting GO was dried overnight at 55 °C to produce the GO powder.

The preparation of functionalized graphene (fG) was carried out using a previously described method.[8] In a typical process, GO was dispersed in dimethylformamide (DMF) by sonication. This solution was heated to 150 °C in an oil batch for different durations, producing fG with different density of functionalities. After reduction, fG was filtrated, washed with ethanol, and dried in vacuum. Five samples were prepared, which were named as fG-1h, fG-2h, fG-3h, fG-4h, fG-6h. The synthesis of benchmark materials, hydrazine reduced GO, was according to the procedure described in Ruoff's work. [2]

2.2. Structural Characterizations

Raman characterization was carried out using a LabRAM ARAMIS, Horiba Jobin Yvon with a 532-nm-wavelength laser. FTIR characterizations were performed at ambient temperature with a FTIR spectrometer (Nicolet, Magna IR 560). Thermogravimetric analysis (TGA) was carried out on a thermogravimetric analyzer (TGA Q5000, TA Instruments Co.). Samples were heated at a rate of 20 °C/min in air. The X-ray photoelectron spectroscopy (XPS) was carried out with a Thermo K-Alpha XPS.

2.3. Electrochemcial Characterizations

The electrochemical properties of fG were tested in a three electrode system. fG was dispersed in N-methyl-2-pyrrolidone (NMP) containing polyvinylidene fluoride (PVDF) as a binder. The ratio between fG and PVDF was 95:5 by weight, and the concentration of electrode materials (fG and PVDF) was 10 mg/mL. To prepare the working electrode, 2.00 μL fG dispersion was transferred onto a glassy carbon electrode (3 mm diameter, 0.07065 cm^2 area) and then dried at 85°C. The fG loading was calculated to be 0.0190 mg. A Pt wire and Ag/AgCl electrode filled with saturated KCl aqueous solution were used as the counter electrode and reference electrode respectively. Prior to the electrochemical test, dissolved oxygen in electrolyte was removed by bubbling N_2 for 10 mins. Cyclic voltammetry (CV) and galvanostatic charge/discharge were measured on a versastat 2-channel system (Princeton Applied Research). The specific capacitance is calculated according to equation: C=It/V, where I is the charge/discharge current density (A/g), t is the discharge time (t), and V is the voltage (0.8 V). The reported specific capacitance and energy density are all normalized to the weight of fG.

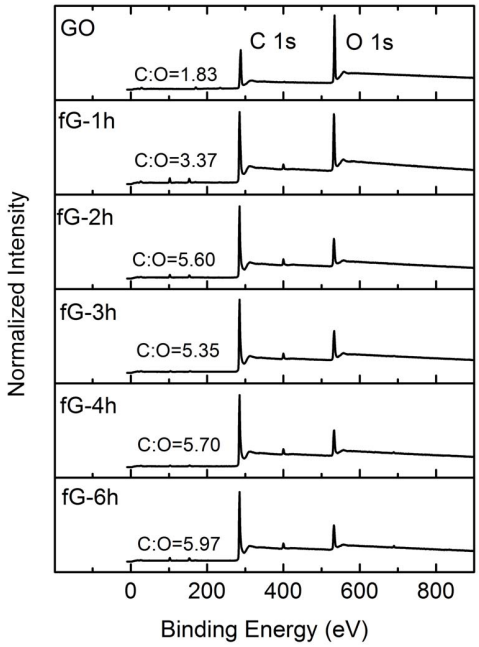

Figure 1. XPS spectra of GO and fGs.

3. Results and Discussion

The reduction of GO during the solvothermal reaction has been studied previously by our group.[8] In this report, GO is solvothermally treated for different durations to control the density of functionalities. Thus fG sample is denoted as fG-time, where time indicates the reaction time (h).

The structure and fG was investigated by a set of structural characterizations, including X-ray photoelectron spectroscopy (XPS), thermal gravimetric analysis (TGA), fourier transform infrared spectroscopy (FTIR) and Raman spectroscopy. Figure 1 shows the XPS spectra of GO and fGs. The peaks of ~ 285 eV and ~ 530 could be attributed to carbon atoms and oxygen atoms respectively. From XPS spectra, the C/O atomic ratios can be calculated, which are listed in Figure 1. For the starting materials GO, the C/O ratio is 1.83, indicating a high content of oxygen. The C/O ratio increases to 3.37 for fG-1h, evidencing a reduction of GO, and continues to increase to 5.60 for fG-2h. However, the C/O ratio does not change much afterwards, suggesting that the solvothermal reaction sucessfully remove oxygen atoms in the first 2-3 hours but is not able to further lower down the oxygen content. Compared to typical reduction of GO using reducing agent, which can achieve C/O up to 10,[9] our method allows a very high retention of oxygen-containing groups.

The TGA curves of GO and fG are shown in Figure 2. GO has a 20.5 % weight loss at ~ 200 °C, due to the decomposition of liable functionalities,[10] and completely

decompose at ~650 °C. The reduction of GO greatly improves the thermal stability, evidenced by less weight losses at ~200 °C for all fG samples. Moreover, it can be seen that the fG-1h is not fully reduced, while other fGs show similar and less weight loss at ~ 200 °C. However, it is interesting that fG-1h exhibit a higher thermal stability at high temperatures, which completely decompose at ~750 °C. In contrast, fG with longer reaction time tend to fully decompose at a lower temperature. For example, fG-6h decomposes completely at a temperature of ~ 700 °C. Considering that the thermal stability of fG is closely related to its structure, we believe that the thermal treatment longer than 2 – 3 hours, instead of removing the oxygen, is able to change the atomic structure of fG.

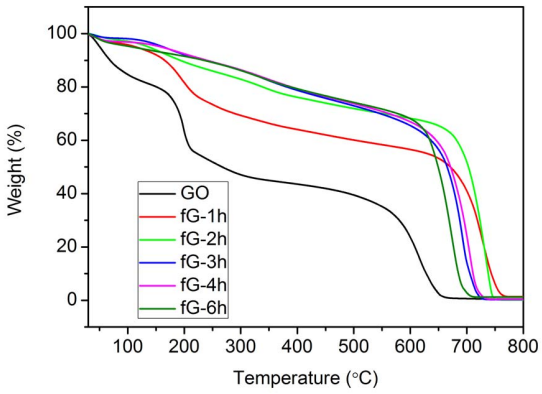

Figure 2. TGA curves of GO and fG. Samples were heated at a rate of 20 °C/min in air.

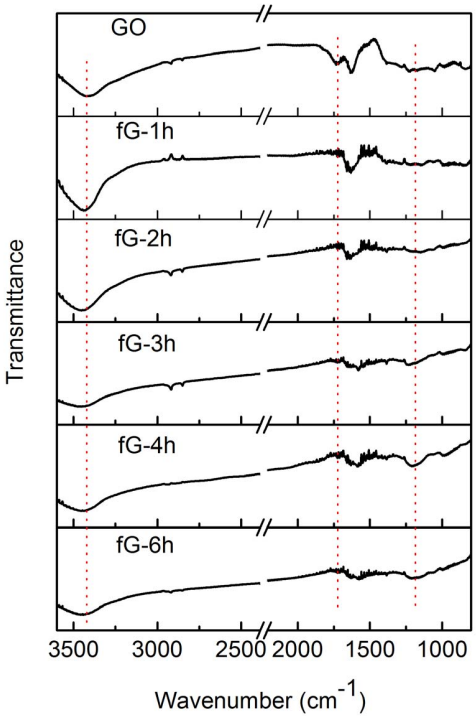

Figure 3. FTIR spectra of GO and fG. Red dash lines indicate the peaks with significant change during the reaction.

The function of solvothermal treatment is further studied by FTIR spectra, which is shown in Figure 3. GO shows distinct peaks ~ 3420 (broad), ~1725, ~1625 cm^{-1}, corresponding to hydroxyls, carbonyls (carboxylic and ketone), and absorbed water respectively.[11] After solvothermal treatment, the ~ 3420 cm^{-1} peak becomes sharper and move to higher wavenumber, and ~ 1725 cm^{-1} peak is diminished. These changes are both due to the decomposition of carboxyls and loss of absorbed water. Moreover, sharp peaks at ~1582 and ~1380 cm^{-1} result from unoxidized aromatic region and hydroxyls respectively, and do not change significantly.[11] Furthermore, the broad peak ~ 1222 cm^{-1} is related to phenolic, epoxy and ketone groups.[11, 12] This peak starts to appear for fG-3h, and become intense for fG-4h and fG-6h, indicating the evolution of atomic structure of fG. Overall, the FTIR results suggest that the reduction of GO is due to the decomposition of mainly carboxylic groups, and the residual functionalities are mainly hydroxyl, ketone and epoxy groups.

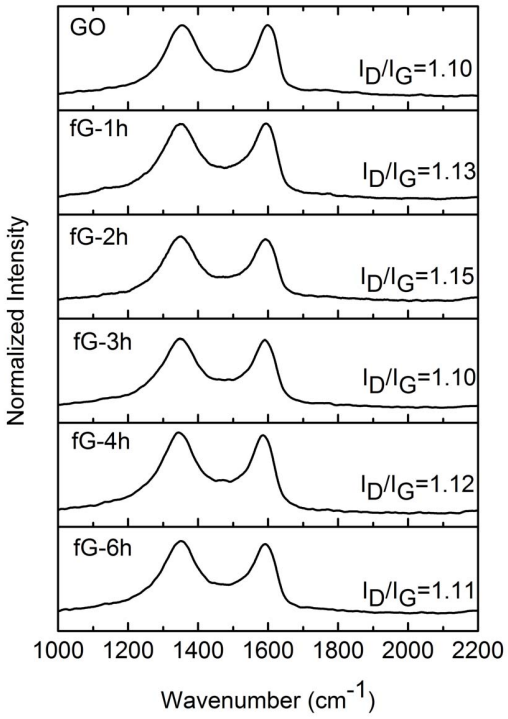

Figure 4. Raman spectra of GO and fG.

Raman spectra shown Figure 4 gives more information about the structure of fG. The I_D/I_G ratio in the Raman of graphene is a measure of the size of nanographite domain.[13] From Figure 4, we can see that the I_D/I_G ratio do not vary much for all samples, showing that the size of nanographite domain does not increase during the reaction. This is possibly because during solvothermal reaction, oxygen-containing groups are released as small gas molecules, such as CO_2 and CO. Thus holes are generated after reduction and the conjugated system is actually not enlarged. The existence of holes in fG is consistent with the theoretical prediction[14]

and experimental observations[15, 16] of the atomic structures of GO and reduced GO.

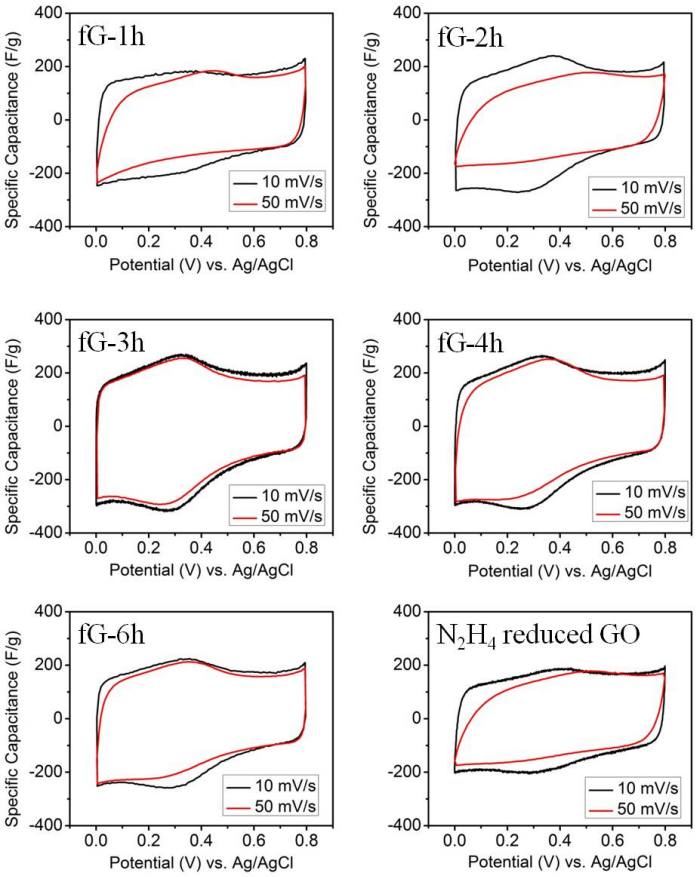

Figure 5. CV curves of fGs. A 1 M H_2SO_4 was used as electrolyte.

Based on these structural characterizations, we believe that surface functionalities in fG are mainly hydroxyl, epoxy, ketone groups as well as holes. The presence of holes in fG-3h, as a special type of functionality, is also important because edges have higher specific capacitance than basal plane.

The capacitive performance of fGs was characterized in a conventional three-electrode system and a 1 M H_2SO_4 was used as the electrolyte. The cyclic voltammetry (CV) curves of fG are shown in Figure 5. At a low scan rate of 10 mV/s, all fG show clear capacitive behaviors with a rectangle-like CV curve. The redox reactions of surface functionalities lead to faradic peaks which can be observed at ~ 0.4 V of anodic scan and ~ 0.35 V of cathodic scan. However, these faradic peaks are not obvious in the case of fG-1h and N_2H_4 reduced GO. For fG-1h, the electrical conductivity is poor which limits the charge migration though the graphene sheet. Thus the pseudocapacitance cannot be fully utilized. For N_2H_4 reduced GO, the low oxygen content is the reason for the absence of large faradic peak.

When increasing the scan rate to 50 mV/s, most CV curves becomes distorted as a result of either poor electrical conductivity or poor wetting property. For fG-1h and fG-2h, the poor electrical conductivity leads to difficulties in utilizing EDLC and pseudocapacitance at high discharge rate. For fG-4h and fG-6h as well as N_2H_4 reduced GO, the surface of graphene sheets is more hydrophobic which limits the wetting with electrolyte. Thus their CV curves derivates from rectangle shape. fG-3h is the only sample maintains rectangle shape at high scan rate of 50 mV/s, due to its acceptable electrical conductivity and wetting property. Furthermore, we would like to mention that the faradic peaks resulting from chemical reactions of surface functionalities are diminished at 50 mV/s, indicating slow charge/discharge kinetics of pseudocapacitance compared to EDLC.

The specific capacitance of fGs can be calculated from galvanostatic discharge curves. The charge/discharge current density varies from 0.1 A/g to 5 A/g. Similar to the result from CV measurement, fG-3h shows a highest specific capacitance up to 276 F/g at 0.1 A/g, which is still as high as 205 F/g at 5 A/g. These values are much higher than 238 F/g and 143 F/g measured for N_2H_4 reduced GO at 0.1 A/g and 5 A/g respectively.

Typical galvanostatic discharge curves of fG-1h, fG-3h and N_2H_4 reduced GO are shown in Figure 6, which gives a informative clue on the influence of electrical conductivity and wetting properties as well as aggregations. It is clear that the discharge curves deviate from ideal linear shape with small specific capacitance at higher potentials and large values at lower potentials. From this result together with CV curves, it can be inferred that the specific capacitance between 0.6 - 0.8 V is mainly due to EDLC, while at lower voltages, the pseudocapacitance becomes dominating.

Figure 6a shows discharge curves measured at a small discharge current of 0.1 A/g. Between 0.6 - 0.8 V, the EDLC of fG-1h is lower than fG-3h and N_2H_4 reduced GO, due to the poor electrical conductivity of fG-1h. Moreover, although fG-3h has higher oxygen content than N_2H_4 reduced GO, it exhibits a similar EDLC value, which signifies that the oxygen-containing groups in fG-3h do not affect the electrical conductivity and thus the utilization of EDLC. At lower voltage, it can be seen that the fG-3h shows larger specific capacitance than N_2H_4 reduced GO, which could be attributed to pseudocapacitance of surface functionalities.

Figure 6b shows the discharge curves measured at large discharge current of 5 A/g. Between 0.6 – 0.8 V, instead of fG-1h, the N_2H_4 reduced GO shows the smallest EDLC. This is because that the severe aggregation and poor wetting property give rises to high ion diffusion resistance. In contrast, fG-3h has more oxygen-containing functional groups and thus less aggregation and better wetting with electrolyte, which lead to a large specific capacitance.

As discussed above, fG-3h shows the highest specific capacitance among fGs tested. More electrochemical characterizations are conducted to evaluate the capacitive performance of fG-3h. Figure 7a shows the rate performance of fG-3h. The value of pseudocapacitance is extracted by subtracting EDLC from overall capacitance assuming a

constant EDLC. The capacitance retention is 74.3 %, 80.5 %, 69.6 % respectively at 5 A/g for overall capacitance, EDLC and pseudocapacitance, which are much higher than typical pseudocapacitive materials such as conducting polymers[5] and metal oxides[4]. Thus it can be inferred that the charge/discharge kinetics of pseudocapacitance in fG-3h is faster than typical pseudocapacitive reactions in graphene/GO supported conducting polymers and metal oxides. Figure 7b is the Ragone plot of fG-3h showing that the specific energy of fG-3h is 20.0 and 14.5 Wh/kg respectively at specific powers of 34.5, and 1.69×10^3 W/kg. The cycling stability of fG-3h was evaluated at a constant charge/discharge current of 1 A/g. As shown in Figure 7c, after 2000 cycles, the specific capacitance of fG-3h, instead of decreasing, increase from ~230 F/g to ~ 250 F/g. From CV curve shown in Figure 7d, we can see stronger faradic peaks after stability test than that before stability test. Therefore, we believe that during stability test, more oxygen containing groups are introduced into fG-3h, which provide more pseoducapacitance.

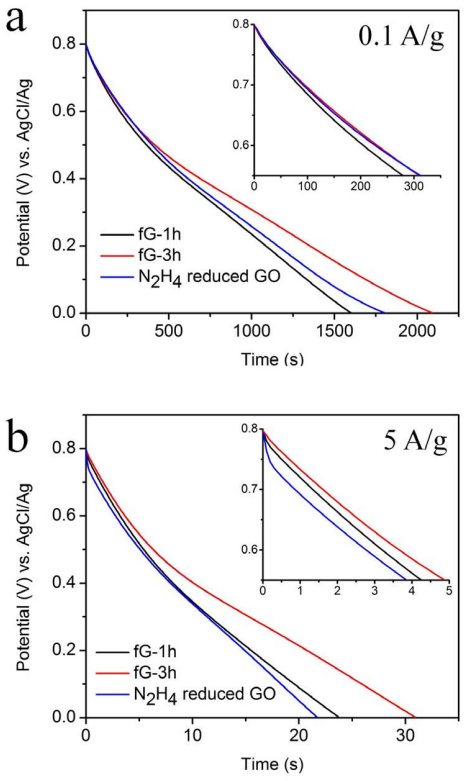

Figure 6. Galvanostatic discharge curves of fG-1h, fG-3h and N_2H_4 reduced GO at (a) 0.1 A/g and (b) 5 A/g. Insets are enlarged curves showing details between 0.6 -0.8 V.

Conclusions

A solvothermal method was used to prepare fGs, which have oxygen-containing groups on graphene sheet. At an optimized condition, a specific capacitance up to 276 F/g can be achieved with good rate performance and cycling stability. The high capacitance is due to the surface oxygen-containing groups, which allows large psudeocapacitacne, less aggregation and good wetting properties. The superior capacitive performance of fG demonstrates the importance of controlling the surface chemistry of graphene for supercapacitor applications.

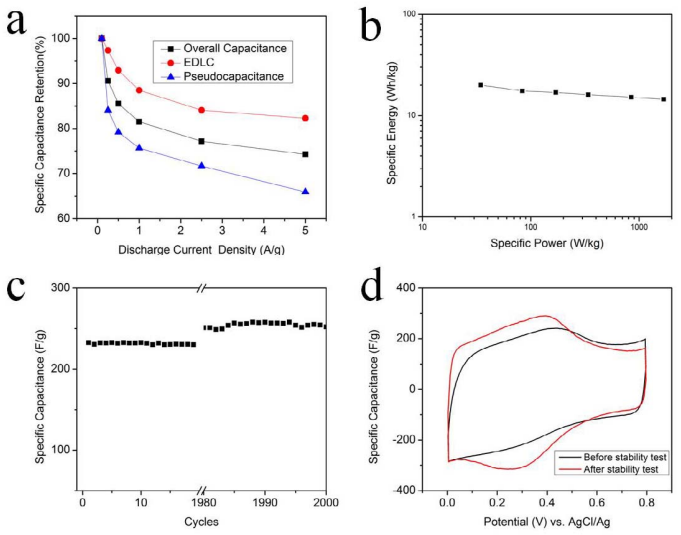

Figure 7. More electrochemical characterizations of fG-3h: (a) rate performance; (b) Ragone plot; (c) stability test at 1 A/g; (d) CV curves before and after stability test.

Acknowledgments

We thank Dr. Albert Tamashauski of Asbury Carbon for generously providing the graphite material.

References

1. P. Simon and Y. Gogotsi, "Materials for electrochemical capacitors," *Nature Materials,* vol. 7,(2008) pp. 845-854.
2. M. D. Stoller, *et al.*, "Graphene-Based Ultracapacitors," *Nano Letters,* vol. 8,(2008) pp. 3498-3502.
3. C. G. Liu, *et al.*, "Graphene-Based Supercapacitor with an Ultrahigh Energy Density," *Nano Letters,* vol. 10,(2010) pp. 4863-4868.
4. S. Chen, *et al.*, "Graphene Oxide-MnO2 Nanocomposites for Supercapacitors," *Acs Nano,* vol. 4,(2010) pp. 2822-2830.
5. K. Zhang, *et al.*, "Graphene/Polyaniline Nanofiber Composites as Supercapacitor Electrodes," *Chemistry of Materials,* vol. 22,(2010) pp. 1392-1401.
6. W. S. Hummers and R. E. Offeman, "Preparation of Graphitic Oxide," *Journal of the American Chemical Society,* vol. 80,(1958) pp. 1339-1339.
7. L. Staudenmaier, "Verfahren zur Darstellung der Graphitsäure," *Berichte der deutschen chemischen Gesellschaft,* vol. 31,(1898) pp. 1481-1487.
8. Z. Lin, *et al.*, "Solvent-Assisted Thermal Reduction of Graphite Oxide," *The Journal of Physical Chemistry C,* vol. 114,(2010) pp. 14819-14825.
9. S. Stankovich, *et al.*, "Synthesis of graphene-based nanosheets via chemical reduction of exfoliated graphite oxide," *Carbon,* vol. 45,(2007) pp. 1558-1565.
10. M. J. McAllister, *et al.*, "Single sheet functionalized graphene by oxidation and thermal expansion of

graphite," *Chemistry of Materials,* vol. 19,(2007) pp. 4396-4404.
11. T. Szabo*, et al.*, "Evolution of surface functional groups in a series of progressively oxidized graphite oxides," *Chemistry of Materials,* vol. 18,(2006) pp. 2740-2749.
12. M. Acik*, et al.*, "The Role of Intercalated Water in Multilayered Graphene Oxide," *Acs Nano,* vol. 4,(2010) pp. 5861-5868.
13. M. A. Pimenta*, et al.*, "Studying disorder in graphite-based systems by Raman spectroscopy," *Physical Chemistry Chemical Physics,* vol. 9,(2007) pp. 1276-1291.
14. A. Bagri*, et al.*, "Stability and Formation Mechanisms of Carbonyl- and Hydroxyl-Decorated Holes in Graphene Oxide," *Journal of Physical Chemistry C,* vol. 114,(2010) pp. 12053-12061.
15. C. Gomez-Navarro*, et al.*, "Atomic Structure of Reduced Graphene Oxide," *Nano Letters,* vol. 10,(2010) pp. 1144-1148.
16. K. Erickson*, et al.*, "Determination of the Local Chemical Structure of Graphene Oxide and Reduced Graphene Oxide," *Advanced Materials,* vol. 22,(2010) pp. 4467-4472.